^{99}Mo AND ^{67}Cu ISOTOPE YIELDS UNDER PRODUCTION CONDITIONS OF NSC KIPT ELECTRON ACCELERATOR KUT-30

N.I. Aizatsky, N.P. Diky, A.N. Dovbnya, D.Ehst[1], Yu.V. Lyashko, V.I. Nikiforov,
A.Eh. Tenishev, A.V. Torgovkin, V.L. Uvarov, V.A. Shevchenko, B.I. Shramenko
National Science Center "Kharkov Institute of Physics and Technology", Kharkov, Ukraine;
[1]Argonne National Laboratory, USA
E-mail: uvarov@kipt.kharkov.ua

Computer simulation has been used to determine the ^{99}Mo and ^{67}Cu isotope yields, as well as the radiation power absorbed in technological natural Mo- and Zn-based targets of different mass and geometry, and also, the power absorbed in a tantalum converter versus the converter thickness and spatial-energy characteristics of the electron beam from the accelerator KUT-30 (energy up to 45 MeV, average beam current up to 300 μA). The results of experimental studies are in good agreement with the simulation data.

PACS: 07.85.-m, 81.40wx, 87.53-j, 87.53.Wz

1. INTRODUCTION

The photonuclear method of isotope production has become the object of practical engineering [1-3]. Its advantages include reliability, a moderate cost of electron accelerators and their operation, and also, the ecological safety. Of particular interest is the production of ^{99}Mo isotope (generator of the basic diagnostic radionuclide ^{99m}Tc) and ^{67}Cu isotope, which is considered as one of the most promising radionuclides for radioimmunotherapy [4].

One of the main problems of photonuclear technology is the conversion of a high-intensity electron beam ($\geq$ 10 kW/cm^2) into a flux of mixed e,X-radiation, which irradiates the target [5]. Therefore, the necessary initial stage of the process development should involve the optimization of the composition and service conditions of the accelerator output devices for providing the maximum yield of the desired isotope with retention of heat resistance of the mentioned devices [3].

The NSC KIPT specialists have created the accelerator KUT-30 as a basic setup for developing the photonuclear technology [6]. The paper presents the results of studies on the ^{99}Mo and ^{67}Cu isotope yields that can be realized with technological targets at KUT-30.

2. SIMULATION OF TARGET ACTIVATION

To calculate the isotope yield and the absorbed radiation power in output device components of the electron accelerator operated in the mode of isotope production, we have used the computer simulation technique based on the package PENELOPE/2006 supplemented with the database of excitation functions for photonuclear reactions [7]. Earlier, this approach has been demonstrated to provide good agreement with the experimental results [4].

2.1. DESCRIPTION OF OUTPUT DEVICES

In simulation, consideration has been given to a variant of output devices (see Fig.1) composed of the bremsstrahlung converter and the target. The converter unit includes the input (1) and output (6) titanium foils, 50 μm in thickness, and a set of tantalum plates (2-5), each being 1 mm thick, placed between the foils. Sets of 3, 4, 5 and 6 plates have been considered.

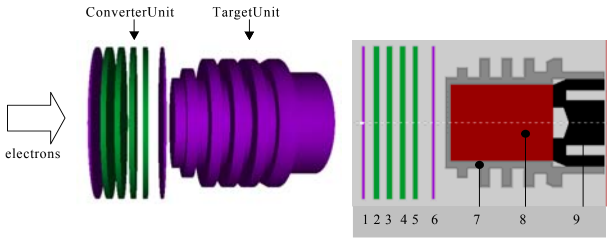

Fig.1. Configuration of accelerator output devices

The arrangement of plates in the space between the foils is uniform in all cases. The spacings between the foils and the plates are filled with cooling water.

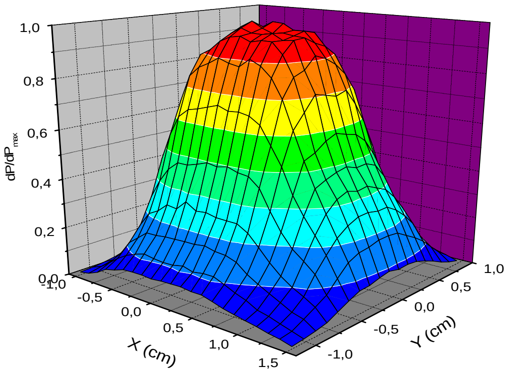

Fig.2. Electron beam density distribution

Two variants of the target device have been investigated: in the 1st variant (see Fig.1) the working substance 8 is located within the titanium capsule 7 in the cylindrical cavity of diameter D=20 mm and height H=19.3 mm. The cavity is sealed with a cap bolt 9. In the 2nd variant, the target is a homogeneous cylinder, which is placed behind the converter and is axially symmetric about the electron beam. In both cases, the devices are surrounded with water.

The electron beam propagates along the horizontal axis Z. The X-axis is directed vertically upwards, and the Y-axis lies horizontally. The XOY plane is coincident with the front wall of the exit-window foil of the accelerator. In the transverse plane electrons have a nonuniform distribution of exit points as indicated by their profiles measured along the X- and Y-axis (see Fig.2). The electron energy distribution also corresponds to the measured spectrum of the accelerator KUT-30 (Fig.3).

2.2. SIMULATION RESULTS

2.2.1. Calculations for the capsule-containing target device (Fig.1) have been performed with the working substance of two types: i) natural molybdenum of density 10.2 g/cm^3 (mass 62 g) with the ^{100}Mo isotope abundance of 9.63%, and ii) molybdenum trioxide in powder form having a bulk density of 2.13 g/cm^3, mass of 12.9 g and the ^{100}Mo isotope abundance of 6.42% (see Table 1).

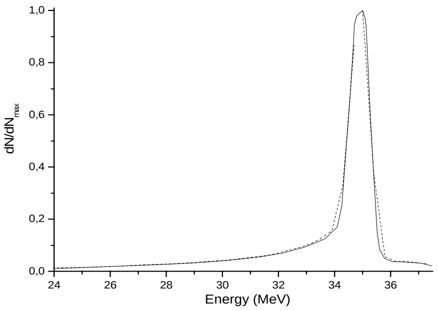

Fig.3. Experimental (solid curve) and simulated (dotted line) beam spectra

Table 1

Simulation results for ^{99}Mo yield from Mo and MoO_3 targets (Ta, 4 mm)

Energy E_0, MeV	Working substance	Absorbed power, kW/mA		^{99}Mo activity	
		Target	Working substance	Total mCi/(100μA·1h)	Specific, mCi/(100μA·g·1h)
35	Mo	5.449 ± 0.019	3.75 ± 0.01	15.90 ± 0.21	0.2565 ± 0.0034
	MoO_3	3.550 ± 0.012	1.237 ± 0.002	1.897 ± 0.023	0.1469 ± 0.0018
40	Mo	7.497 ± 0.027	5.24 ± 0.02	20.34 ± 0.23	0.3283 ± 0.0038
	MoO_3	4.858 ± 0.017	1.667 ± 0.001	2.407 ± 0.026	0.1863 ± 0.0020

Fig.4 shows the ^{99}Mo yield versus target mass at different target diameter-height ratios. For each target mass value the diameter D_0 is determined from the condition D_0=H.

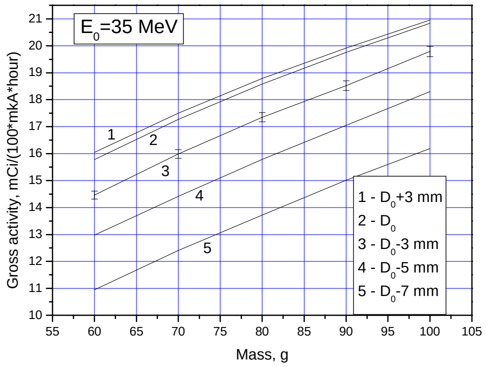

Fig.4. Activity of cylindrical Mo targets of different masses and dimensions

The ^{99}Mo yield and the absorbed radiation power in the cylindrical natural molybdenum target (15 mm in diameter, 16.6 mm in height and 30 g in mass) were also investigated as functions of the number of Ta-converter plates (Fig.5, Table 2).

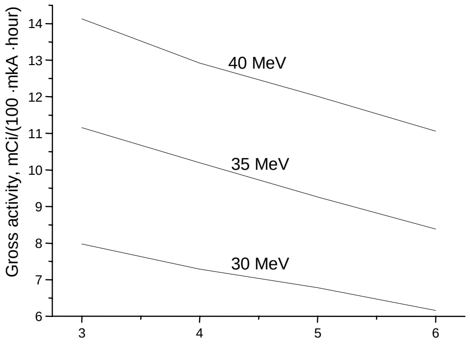

Fig.5. Mo-99 yield versus converter thickness

Table 2

Absorbed power in the Mo target (30 g) and its activity at different Ta-converter thickness and electron energy values

Energy E_0, MeV		30	35	40
3 mm converter	P, W/μA	2.368	3.407	4.577
	A, μCi/μA·h	79.72	111.6	141.3
4 mm converter	P, W/μA	1.607	2.455	3.395
	A, μCi/μA·h	72.89	102.0	129.2
5 mm converter	P, W/μA	1.205	1.842	2.634
	A, μCi/μA·h	67.78	92.60	120.1
6 mm converter	P, W/μA	0.989	1.488	2.085
	A, μCi/μA·h	61.56	83.79	110.6

2.2.2. Preliminary studies have shown that for photonuclear production of Cu-67 isotope by the reaction $^{68}Zn(\gamma,p)^{67}Cu$ the 2×2 cm cylinder is the optimum target as regards the total-to-specific activity ratio [3]. Figs.6,7 and Table 3 show the Cu-67 yield from this target versus converter thickness for different E_0 values, and also the data on absorbed power in both the target and the converter.

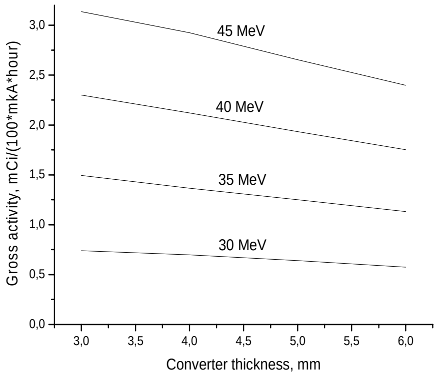

Fig.6. Cu-67 yield versus converter thickness

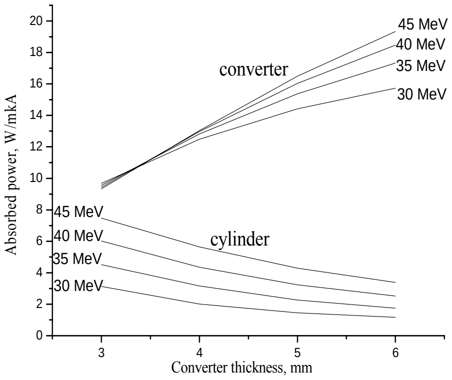

Fig.7. Absorbed radiation power in the converter and in the Zn target versus converter thickness

Table 3

Absorbed power in the Zn target and its activity at different converter thickness and electron energy values

EnergyE_0, MeV		30	35	40	45
3 mm conv.	P, W/μA	3.135	4.508	6.022	7.466
	A, μCi/μA·h	7.400	14.94	23.00	31.37
4 mm conv.	P, W/μA	2.015	3.153	4.351	5.639
	A, μCi/μA·h	6.987	13.65	21.20	29.25
5 mm conv.	P, W/μA	1.448	2.265	3.234	4.288
	A, μCi/μA·h	6.405	12.51	19.32	26.54
6 mm conv.	P, W/μA	1.172	1.737	2.522	3.391
	A, μCi/μA·h	5.741	11.32	17.52	23.98

3. EXPERIMENTAL STUDIES ON ISOTOPE YIELDS

3.1. TARGET DEVICES

To test the photonuclear activation conditions, a few variants of target devices have been designed (Fig.8):

- device No 1 for short-term activation of targets with moderate induced activity for diagnostics of irradiation conditions (Fig.8,a);
- base target No 2 for specifying the process conditions of activation (Fig.8,b);
- capsule No 3 for exposure of powder targets (Fig.8,c).

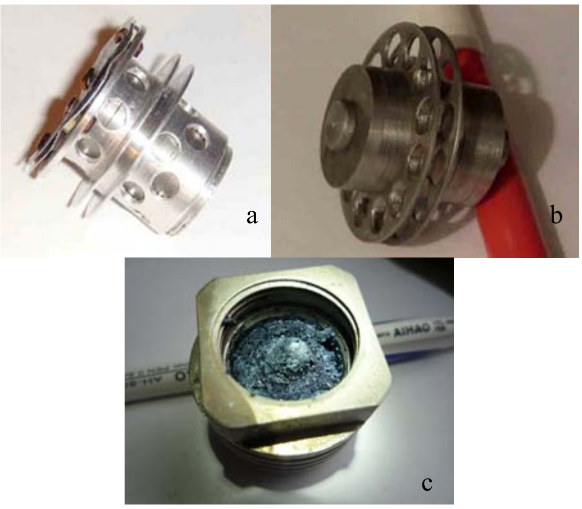

Fig.8. Target device variants

Target No1 accommodated a set of ten Mo discs, each of diameter 19 mm and thickness 2 mm. Between the discs there were placed 10 Mo foils (Ø19 mm, thickness – 90 μm, m≈240 mg – Mo-19 (1)…Mo-19 (10)). The foils were used to analyze the induced activity distribution along the target axis. The whole molybdenum assembly, 59.2 g in mass, was placed into an aluminum cassette ribbed to hold the target behind the converter and to provide additional cooling of the cassette. The cassette body had openings for admitting water. The front part of the cassette also comprised Mo and Sn foils-monitors, 34 mm in diameter (Fig.9). From the Mo-monitor activity ratio $A_{Mo-19(1)}\big/A_{Mo-34}$ the coefficient of "bremsstrahlung utilization" by the target has been estimated. The Sn monitor was used to measure the bremsstrahlung flux profile on the target by the photonuclear converter technique [9]. Target No 2, including the ribs, was fully made from Mo.

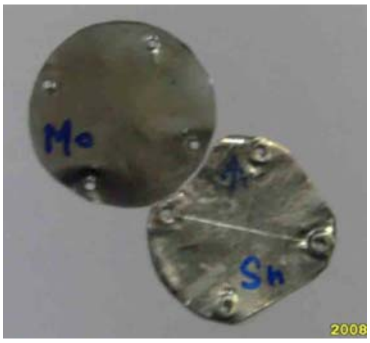

Fig.9. Foils-monitors of bremsstrahlung profile

To measure the photonuclear yield of Cu-67 and its distribution along the target axis, 20 natural-zinc discs, each being 1 mm thick, were placed into device No 1.

3.2. RESULTS

3.2.1. The target devices were tested in the mode of ^{99}Mo and ^{67}Cu generation at the following beam parameters:

electron energy, MeV	36;
pulse length, μs	3.2;
pulse-repetition frequency, Hz	150;
average beam current, μA	260.

Figure 10 shows the profile of high-energy bremsstrahlung flux behind the converter, which was obtained by measuring the Sn-monitor surface activity distribution using of a gamma-scanner [9].

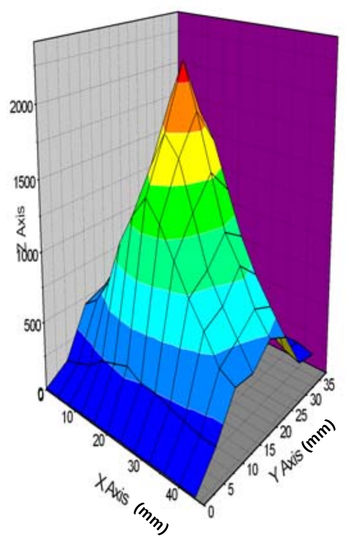

Fig.10. Pprofile of high-energy bremsstrahlung flux

3.2.2. For the analysis of radionuclide composition and target activity, the spectrometric system “CANBERRA” was used. Its energy resolution in the 1332 keV γ-line was 2 keV. To determine the contribution of short-lived isotopes to the total activity, the Mo-19(2) sample was measured 2 hours after exposure (EOB). The obtained results are presented in Table 4.

Table 4

Mo-19(2) sample activity characteristics (after EOB)

Isotope	T (1/2)	Specific activity (t=0), mCi/g·100μA ·1h	Ratio to desired isotope, %
Mo-99	66 hour	2.71E-01	100
Nb-95	35 days	0.63E-03	0.2
Nb-95m	86.6 hour	1.095E-02	4.0
Nb-96	23.3 hour	3.55E-02	13.1
Mo-90	5.67 hour	3.44E-02	12.7
Nb-90	14.6 hour	2.12E-02	7.8
Nb-97	74 min	1.175E+00	432.6
Nb-98m	51.3min	0.92E-02	3.4

A comparison between the measured specific activity of ^{99}Mo and its calculated values (see Table 1) shows their rather good agreement.

Table 5 lists the measured activity values of the zinc disc being the first in the irradiated assembly as viewed from the converter, and Fig.11 shows the ^{67}Cu activity distribution in the depth of the target. As in the ^{99}Mo case, fair agreement has been obtained between the experimental data on the ^{67}Cu yield (Table 5) and the simulation results (Table 3).

Table 5

Zn sample activity characteristics

Радионуклид	$T_{1/2}$ (сут.)	A (мКи/г·100 мкА·1ч)
^{65}Zn	243.2	1,42E-02
^{67}Cu	2.58	6,8E-02
^{69m}Zn	0.573	2,82E-02

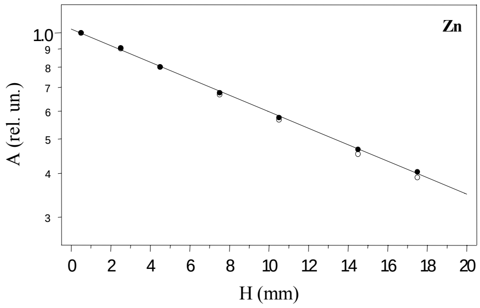

Fig.11. Zn disc activity versus depth in the target device

It should be also noted that with the accelerator KUT-30 operation at an average current of 260 μA (beam power is 9.2 kW) the Ta converter and the water-cooled target device casings have demonstrated (in appearance) good heat resistance at both short- (10 minutes) and long-term (135 minutes) exposure, i.e., at steady temperature conditions as well. Under the same conditions, the MoO_3 powder in the capsule was sintered into a grey-greenish bulk showing color and hardness variations on a radius round the capsule cavity.

CONCLUSION

1. The undertaken studies have demonstrated a fair agreement between the experimental data on the photonuclear isotope yield in technological targets and the results of simulation based on a modified program system PENELOPE/2006.

2. The NSC KIPT electron linear accelerator KUT-30, operated in the (36 MeV, 260 μA) mode, can provide the production of ^{99}Mo and ^{67}Cu isotopes in amounts up to 1 Ci and 150 mCi for a day, respectively, with the use of molybdenum (30 g) and zinc (42 g) targets of natural isotopic composition. In the targets of similar masses, but enriched in ^{100}Mo and ^{68}Zn, the daily yield can attain 10 Ci for ^{99}Mo and 800 mCi for ^{67}Cu. In all the cases, provision should be made for an efficient cooling of targets. The present data (Tables 2, 3) enable one to specify the optimum conditions of target activation, which would provide the maximum yield of the desired isotope with retention of heat resistance of the target.

3. On retention of accelerator beam parameters, an additional yield of desired isotopes can be attained by increasing the target mass, however in this case the target specific activity would decrease. The maximum ^{99}Mo yield in the cylindrical Mo target of given mass is attained at close values of its diameter and height. As calculations indicate, in the ^{67}Cu case this ratio switches to a greater target height.

4. For photonuclear production of the ^{99}Mo/^{99m}Tc isotope the MoO_3-base target is of little use with regard to both the desired isotope yield and its heat resistance.

The work has been done partially due to STCU Grant #P228.

ЛИТЕРАТУРА

1. N.P. Dikiy, A.N. Dovbnya, V.L.Uvarov. The Fundamentals of ^{99m}Tc Production Cycle at Electron Accelerator // *Problems of Atomic Science and Technology. Series: Nuclear Physics Investigations.* 2004, №1(42), p.168-171.
2. S. Koscnielniak, P. Bricault, B. Davids, et al. Proposal for a ½ MW Electron Linac for Rare Isotope and Material Science // *Proc. of the 11-th Europ. Part. Accel. Conf. (EPAC’08). Genova, Italy,* 2008, p.985-987.
3. A.N. Dovbnya, V.I. Nikiforov, V.L.Uvarov, V.F.Zhyglo. Optimization of electron linac operating conditions for photonuclear isotope production // *Proc. of the 11th Europian Part. Accel. Conf. (EPAC 08). Genova, Italy,* 2008, p.1308-1310.
4. N.I. Aizatsky, N.P. Diky, A.N. Dovbnya, et al. Peculiarities of photonuclear Cu-67 production. (In Russian) // *Problems of Atomic Science and Technology. Series: Nuclear Physics Investigations.* 2008, №3(49), p.174-178.
5. V.I. Nikiforov, V.L. Uvarov. Analysis of Mixed e,X-Radiation Along the Extraction Facilities of Electron Accelerators // *Atomic Energy.* 2009, v.106, №4, p.281-286.
6. M.I. Ayzatskiy, E.Z. Biller, V.N. Boriskin, et al. High-Power Electron S-band Linac for Industrial

Purposes // *Proc. of the 2003 PAC, Portland, Oregon, USA.* 2003, p.2878-2880.

7. F. Salvat, J.M. Fernandez-Varea and J. Sempau. "PENELOPE-2006 A Code System for Monte Carlo Simulation of Electron and Photon Transport" *(OECD Nuclear Energy Agency, Issyles-Moulineaux, France, 2006)*
8. M.P. Zykov, G.E. Kodina. Methods of ^{99}Mo production (survey) (In Russian) // *Radiokhimiya.* 1999, v.41, №3, p.193-204.
9. V.I. Nikiforov, R.I. Pomatsalyuk, A.Eh. Tenishev, et al. A system for measuring high-energy bremsstrahlung flux profile. (In Russian) // *Problems of Atomic Science and Technology. Series: Nuclear Physics Investigations.* 2008, №3(49), p.196-200.

Статья поступила в редакцию 05.02.2010 г.

ВЫХОД ИЗОТОПОВ ^{99}Mo И ^{67}Cu В УСЛОВИЯХ ПРОИЗВОДСТВА НА УСКОРИТЕЛЕ ЭЛЕКТРОНОВ КУТ-30 ННЦ ХФТИ

Н.И. Айзацкий, Н.П. Дикий, А.Н. Довбня, Ю.В. Ляшко, В.И. Никифоров, А.Э. Тенишев, А.В. Торговкин, В.Л. Уваров, В.А. Шевченко, Б.И. Шраменко, D. Ehst

Методом компьютерного моделирования определены выход изотопов ^{99}Mo, ^{67}Cu и поглощенная мощность излучения в технологических мишенях различной массы и геометрии на основе природных Mo и Zn, а также поглощенная мощность в конвертере из тантала в зависимости от толщины конвертера и пространственно-энергетических характеристик пучка электронов ускорителя КУТ-30 (энергия – до 45 МэВ, средний ток – до 300 мкА). Результаты экспериментального исследования находятся в удовлетворительном соответствии с данными моделирования.

ВИХІД ІЗОТОПІВ ^{99}Mo ТА ^{67}Cu В УМОВАХ ВИРОБНИЦТВА НА ПРИСКОРЮВАЧІ ЕЛЕКТРОНІВ КУТ-30 ННЦ ХФТІ

М.І. Айзацький, М.П. Дикий, А.М. Довбня, Ю.В. Ляшко, В.І. Нікіфоров, А.Е. Тєнішев, О.В. Торговкін, В.Л. Уваров, В.А. Шевченко, Б.І. Шраменко, D. Ehst

Методом комп'ютерного моделювання визначено вихід ізотопів ^{99}Mo, ^{67}Cu і поглинута потужність випромінення в технологічних мішенях різної маси і геометрії на основі природних Mo і Zn, а також поглинута потужність у конвертері з танталу в залежності від товщини конвертера і просторово-енергетичних характеристик пучка електронів прискорювача КУТ-30 (енергія – до 45 МеВ, середній струм – до 300 мкА). Результати експериментального дослідження знаходяться в задовільній відповідності з даними моделювання.